Journal of Solid State Chemistry 182 (2009) 1867–1871

Contents lists available at ScienceDirect

Journal of Solid State Chemistry

journal homepage: www.elsevier.com/locate/jssc

$[Hg_5O_2(OH)_4][(UO_2)_2(AsO_4)_2]$: A complex mercury(II) uranyl arsenate

Yaqin Yu [c], Kai Jiang [c], Thomas E. Albrecht-Schmitt [a,b,c,*]

[a] Department of Civil Engineering and Geological Sciences, University of Notre Dame, Notre Dame, Indiana 46556, USA
[b] Department of Chemistry and Biochemistry, University of Notre Dame, Notre Dame, Indiana 46556, USA
[c] Department of Chemistry and Biochemistry, and Center for Actinide Science, Auburn University, Auburn, Alabama 36849, USA

ARTICLE INFO

Article history:
Received 12 December 2008
Received in revised form
17 March 2009
Accepted 26 March 2009
Available online 8 April 2009

Keywords:
Uranyl arsenate
Transition metal uranyl arsenate
Hydrothermal synthesis and crystal growth

ABSTRACT

Under mild hydrothermal conditions $UO_2(NO_3)_2 \cdot 6H_2O$, $Hg_2(NO_3)_2 \cdot 2H_2O$, and $Na_2HAsO_4 \cdot 7H_2O$ react to form $[Hg_5O_2(OH)_4][(UO_2)_2(AsO_4)_2]$ (**HgUAs-1**). Single crystal X-ray diffraction experiments reveal that **HgUAs-1** possesses a pseudo-layered structure consisting of two types of layers: $^2_\infty[Hg_5O_2(OH)_4]^{2+}$ and $^2_\infty[(UO_2)_2(AsO_4)_2]^{2-}$. The $^2_\infty[Hg_5O_2(OH)_4]^{2+}$ layers are complex, and contain three crystallographically unique Hg centers. The coordination environments and bond–valence sum calculations indicate that the Hg centers are divalent. The $^2_\infty[(UO_2)_2(AsO_4)_2]^{2-}$ layers belong to the Johannite topological family. The $^2_\infty[Hg_5O_2(OH)_4]^{2+}$ and $^2_\infty[(UO_2)_2(AsO_4)_2]^{2-}$ layers are linked to each other through μ_2-O bridges that include Hg···O = U = O interactions.

1. Introduction

Uranyl arsenates display remarkably rich crystal chemistry that can be attributed in part to the structural versatility of U(VI), which generally occurs as tetragonal, pentagonal, and hexagonal bipyramids [1–8]. The formation of extended structures containing uranyl polyhedra usually arises only through the equatorial positions owing to the terminal nature of the apical positions, which typically yields two-dimensional structures [9]. There are some recent examples of interactions between uranyl cations that make use of the apical oxygen atoms, but these are exceedingly rare [10,11].

Of late there has been interest in expanding structural diversity and physico-chemical properties of uranyl phosphates and arsenates through the incorporation of main group elements and transition metals [12–14]. One possibility is that the second metal center could display mixed-valence on a stoichiometric level, but this has yet to be observed in compounds in this class. However, the occurrence of this feature might lead to versatile functional materials with atypical magnetic behavior [15,16]. An unusual and understudied choice for a metal that might display this behavior is mercury. Only a few crystal structures of synthetic Hg(I) compounds have been reported (e.g. $(Hg_2)_2(OH)(NO_3)_3$ and $(Hg_2)_5(OH)_4(NO_3)_6$) [17,18], several Hg(I) minerals are also known [19,20]. The mixed-valence compounds $Hg_4O_2(NO_3)_2$, $Hg^I_2(OH)(NO_3) \cdot Hg^{II}O$, and $(Hg_2)Hg(OH)_2(ClO_4)_2$ have also been structurally characterized [21,22]. Hg^I compounds typically contain $[Hg_2]^{2+}$ units that possess a Hg–Hg single bond with a bong length of approximate 2.53 Å [23], which allows one to partially distinguish Hg(I) from Hg(II) compounds [23]. Some of these aforementioned structural features have been combined into a single compound, namely $[Hg_5O_2(OH)_4][(UO_2)_2(AsO_4)_2]$ (**HgUAs-1**), which is discussed in this work.

2. Experimental

Synthesis: $UO_2(NO_3)_2 \cdot 6H_2O$ (98%, Alfa Aesar), $Hg_2(NO_3)_2 \cdot 2H_2O$ (98.5%, Baker), $Na_2HAsO_4 \cdot 7H_2O$ (99.9%, Baker), and $(CH_3)_4NCl$ (97%, Aldrich), were used as received. Reactions were carried out in PTFE-lined Parr 4749 autoclaves with a 23 mL internal volume. Distilled and millipore filtered water with a resistance of 18.2 MΩ cm was used in the reactions. Standard precautions were performed for handling radioactive materials during work with $UO_2(NO_3)_2 \cdot 6H_2O$ and the products of the reactions. Semi-quantitative EDX analysis was performed using a JEOL 7000F.

$[Hg_5O_2(OH)_4][(UO_2)_2(AsO_4)_2]$ (**HgUAs-1**). $UO_2(NO_3)_2 \cdot 6H_2O$ (0.194 g, 0.388 mmol), $Na_2HAsO_4 \cdot 7H_2O$ (0.0612 g, 0.196 mmol), $Hg_2(NO_3)_2 \cdot 2H_2O$ (0.220 g, 0.695 mmol), $(CH_3)_4NCl$ (0.0215 g, 0.196 mmol), and 2 mL of water were loaded into a 23 mL autoclave. The autoclave was sealed and heated to 200 °C in a box furnace for three days. The autoclave was then cooled at an average rate of 9 °C/h to 35 °C. Initial pH = 1.63 and ending pH = 1.95. Yellow blocks of **HgUAs-1** were recovered and thoroughly washed with water, then rinsed with methanol, and

* Corresponding author at: Department of Chemistry and Biochemistry, and Center for Actinide Science, Auburn University, Auburn, Alabama 36849, USA. Fax: +1 334 844 6959.
E-mail address: albreth@auburn.edu (T.E. Albrecht-Schmitt).

0022-4596/$ - see front matter © 2009 Elsevier Inc. All rights reserved.
doi:10.1016/j.jssc.2009.03.032

allowed to dry. Yield: 146 mg, 19.4% based on uranium. EDX analysis confirmed the presence of Hg, U, and As in the crystals.

Crystallographic studies: A single crystal of **HgUAs-1** was mounted on a thin glass fiber and optically aligned on a Bruker APEX CCD X-ray diffractometer using a digital camera. Initial intensity measurements were performed using graphite monochromated Mo$K\alpha$ ($\lambda = 0.71073$ Å) radiation from a sealed tube and monocapillary collimator. SMART (v 5.624) was used for preliminary determination of the cell constants and data collection control. The intensities of reflections of a sphere were collected by a combination of three sets of exposures (frames). Each set had a different ϕ angle for the crystal and each exposure covered a range of 0.3° in ω. A total of 1800 frames were collected with an exposure time per frame of 30 s.

For **HgUAs-1**, determination of integrated intensities and global refinement were performed with the Bruker SAINT (v 6.02) software package using a narrow-frame integration algorithm. A face-indexed numerical absorption correction was initially applied using XPREP, where individual shells of unmerged data were corrected [24]. The absorption coefficient of this compound is very large, and the moderate residuals are probably the result of a somewhat inadequate absorption correction. These files were subsequently treated with a semi-empirical absorption correction by SADABS [25]. The program suite SHELXTL (v 6.12) was used for space group determination (XPREP), direct methods structure solution (XS), and least-squares refinement (XL) [24]. The final refinement included anisotropic displacement parameters for all atoms. Some crystallographic details are given in Table 1. Additional details can be found in the Supporting information.

Raman spectroscopy: The Raman spectrum of **HgUAs-1** was acquired from a single crystal using a Renishaw inVia Confocal Raman microscope with a 514 nm Ar^+ laser.

Fluorescence spectroscopy: The fluorescence spectrum of **HgUAs-1** was acquired using a PI Acton spectrometer (SpectraPro SP 2356, Acton, NJ) that is connected to the side port of an epi-fluorescence microscope (Nikon TE-2000U, Japan). The emission signal was recorded by a back-illuminated digital CCD camera (PI Acton PIXIS:400B, Acton, NJ) operated by a PC. For all the three compounds examined, the excitation was generated by a mercury lamp (X-Cite 120, EXFO, Ontario, Canada) filtered by a band-pass filter at 450–490 nm. The emission signal was filtered by a long-pass filter with a cutoff wavelength of 515 nm.

Table 1
Crystallographic data for $[Hg_5O_2(OH)_4][(UO_2)_2(AsO_4)_2]$ (**HgUAs–1**).

Compound	$[Hg_5O_2(OH)_4][(UO_2)_2(AsO_4)_2]$
Formula mass	1923
Color and habit	Yellow, block
Space group	$P\bar{1}$
a (Å)	6.8229(5)
b (Å)	6.8795(5)
c (Å)	9.5959(6)
α (deg)	109.456(1)
β (deg)	104.834(1)
γ (deg)	93.867(1)
V (Å^3)	404.74(5)
Z	1
T (K)	193
λ (Å)	0.71073
Maximum 2θ (deg)	28.30
ρ_{calcd} (g cm^{-3})	7.864
μ (Mo$K\alpha$) (cm^{-1})	713.12
$R(F)$ for $F_o^2 > 2\sigma(F_o^2)$[a]	0.0555
$R_w(F_o^2)$[b]	0.1349

[a] $R(F) = \sum ||F_o| - |F_c|| / \sum |F_o|$.
[b] $R_w(F_o^2) = [\sum[w(F_o^2 - F_c^2)^2] / \sum wF_o^4]^{1/2}$.

3. Results and discussion

Structure of $[Hg_5O_2(OH)_4][(UO_2)_2(AsO_4)_2]$ (HgUAs-1): **HgUAs-1** possesses a pseudo-layered structure with $^2_\infty[Hg_5O_2(OH)_4]^{2+}$ and $^2_\infty[(UO_2)_2(AsO_4)_2]^{2-}$ layers. The latter layers consist of UO_7 pentagonal bipyramids that are linked into edge-sharing dimers that are joined together by AsO_4^{3-} tetrahedra. The former layers formulated as $^2_\infty[Hg_5O_2(OH)_4]^{2+}$ consists of three crystallographically unique mercury centers and a mixture of oxo and hydroxo groups. As shown in Fig. 1, the compact three-dimensional structure is constructed by the joining of these layers by bridging oxo atoms, which provide linkages for As(1)···Hg(3), Hg(2)···U(1), As(1)···Hg(3), and U(1)···Hg(3). Fig. 2 shows the interactions of the UO_2^{2+} cations and Hg(1) that provides one method for interconnecting the layers. Previous reports show that the apical (uranyl) vertices of the uranyl bipyramids can be shared with polyhedra containing higher-valence cations, even though this would over-bond the oxygen position [13]. However, long uranyl oxo interactions with interlayer cations are well

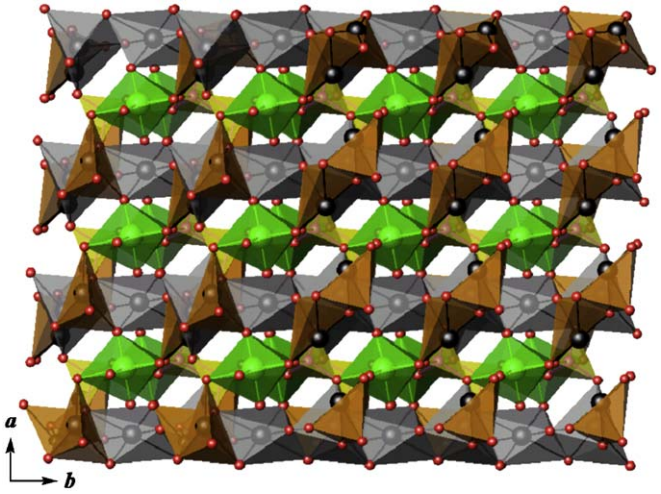

Fig. 1. A view of the three-dimensional structure of $[Hg_5O_2(OH)_4][(UO_2)_2(AsO_4)_2]$ (**HgUAs-1**). UO_7 pentagonal bipyramids are shown in green, Hg polyhedra are shown in gray and brown. AsO_4 tetrahedra are shown in yellow. [For interpretation of the references to color in this figure legend, the reader is referred to the webversion of this article.]

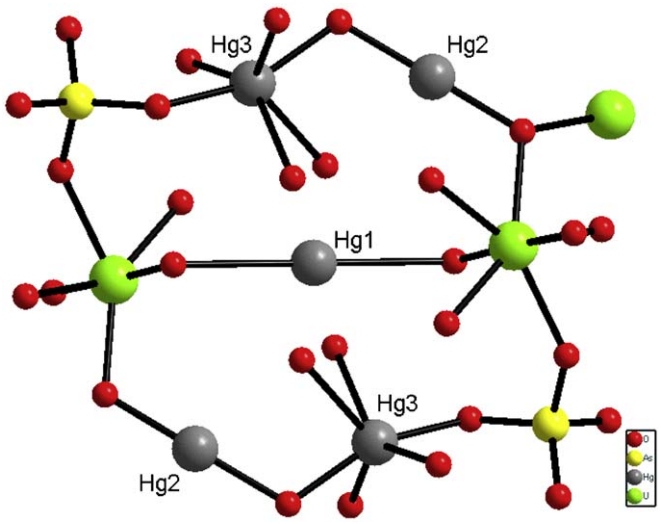

Fig. 2. A depiction of the coordination environments for mercury in $[Hg_5O_2(OH)_4][(UO_2)_2(AsO_4)_2]$ (**HgUAs-1**).

represented [13]. The apical (uranyl) oxygen O(9) provides the μ_2 oxygen atom that bridges to Hg(1).

There is only one crystallographically unique uranium center contained in a nearly linear uranyl, UO_2^{2+}, core in the structure of **HgUAs-1**. The U = O bond lengths are 1.804(14) and 1.835 (15) Å, whereas those in the equatorial plane range from 2.270(13) to 2.371(12) Å. These distances can be used to determine the bond–valence sum of U(1) to be 6.02 [26], which is consistent with the expected oxidation state of U(VI) in UO_2^{2+}. The two-dimensional uranyl arsenate plane of **HgUAs-1** shares some common structural building features with previous members of the Johannite-class of uranyl minerals that are constructed from $UO_2^{2+}/M/SO_4(CrO_4)$ [9]. The most obvious similarity is found in the edge-sharing dimers of UO_7 pentagonal bipyramids that are linked by anions, as shown in Fig. 3. This unit is also found in $Cu[(UO_2)_2(SO_4)_2(OH)_2](H_2O)_8$ and $Sr[(UO_2)_2(CrO_4)_2(OH)_2](H_2O)_8$ [9,27].

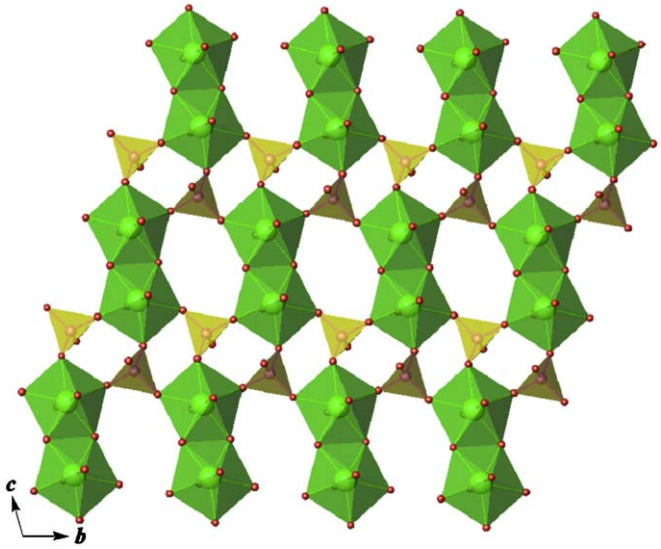

Fig. 3. A view in the [*bc*] plane of the $^2_\infty[(UO_2)_2(AsO_4)_2]^{2-}$ layers with the Johannite topology in $[Hg_5O_2(OH)_4][(UO_2)_2(AsO_4)_2]$ (**HgUAs-1**).

The single arsenic center is found as an AsO_4^{3-} distorted tetrahedron. The As–O bond distances average is 1.689(13) Å; yielding a reasonable bond–valence sum for As(V) of 4.95 [28–30]. However, this average encompasses both short and long As–O bonds. An As-OH moiety is typically indicated by longer, terminal As–O bonds; these are not present. Three oxygen vertices of the AsO_4 tetrahedron are shared with uranyl or mercury. The remaining As(1)–O(1) bond is terminal and short, with a bond distance of 1.661(12) Å indicating an As = O unit [8,31].

The most intriguing feature of this compound is the $^2_\infty[Hg_5O_2(OH)_4]^{2+}$ layer shown in Fig. 4. There are three crystallographically unique mercury centers. In each case there are two short Hg–O bonds and a series of longer interactions listed in Table 2. Hg(1) and Hg(2) can be described as linear if these longer interactions are excluded, but Hg(3) cannot be described in this fashion because the two short Hg–O bonds are not trans to one another. Bond–valence sum calculations indicate that these longer interactions are important for stabilizing a divalent oxidation state for all three Hg centers, with values ranging from 1.75 to 1.82 [29–31]. In addition to these bond–valence sums, the absence of short Hg···Hg contacts indicates that this is not a Hg(I) compound. This is important because charge balance considerations point to the presence of a mixture of hydroxo and oxo groups in these layers Table 3.

Raman spectroscopy: The Raman spectrum of **HgUAs-1** is shown in Fig. 5. The band at 804 cm^{-1} is attributed to the ν_1 symmetric stretching mode for the UO_2^{2+} unit. However, this band is in close proximity with several AsO_4^{3-} modes. The empirical relationship provided by Bartlett and Cooney ($R = 106.5[\nu_1(UO_2)^{2+}]^{-2/3}+0.575$ Å) enables us to calculate the U = O bond lengths in uranyl units of **HgUAs-1** using the Raman shift of the uranyl symmetric stretching vibrations $[R(Å)/\nu_1(cm^{-1})] =$ 804 cm^{-1}, yielding a bond length of 1.804 Å, which is reasonably

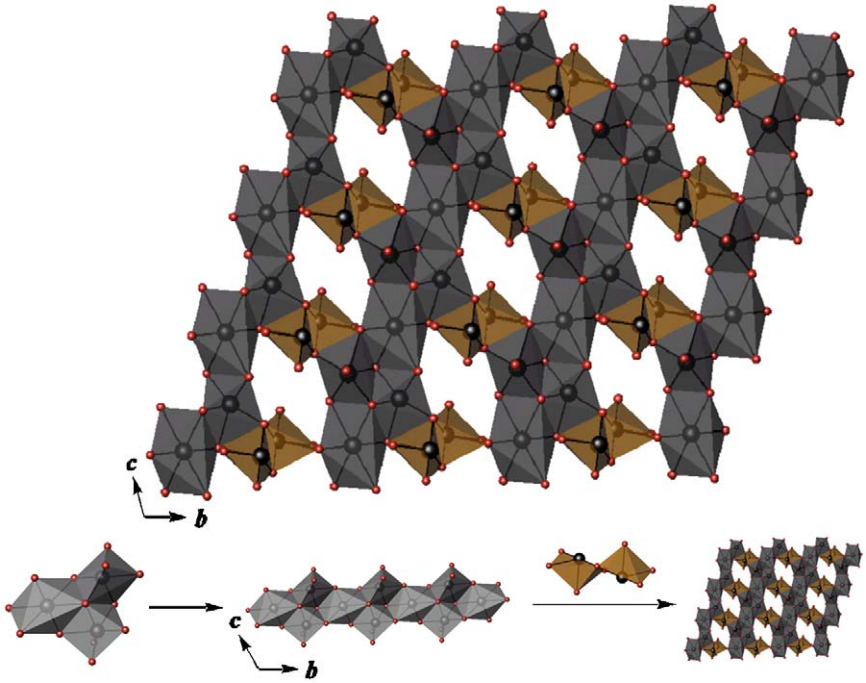

Fig. 4. A view in the [*bc*] plane of the $^2_\infty[Hg_5O_2(OH)_4]^{2+}$ layers in $[Hg_5O_2(OH)_4][(UO_2)_2(AsO_4)_2]$ (**HgUAs-1**). The lower portion of the figure shows how these layers are constructed from the three crystallographically unique Hg(II) centers.

Table 2
Selected bond distances (Å) and angles (deg) for $[Hg_5O_2(OH)_4][(UO_2)_2(AsO_4)_2]$ (**HgUAs-1**).

Distances (Å)			
U(1)–O(9)	1.804(14)	Hg(2)–O(6)	2.074(13)
U(1)–O(8)	1.835(15)	Hg(3)–O(4)	2.130(12)
U(1)–O(7)♯2	2.270(13)	Hg(3)–O(6)	2.147(13)
U(1)–O(7)	2.303(14)	Hg(3)–O(5)	2.468(13)
U(1)–O(1)♯3	2.315(13)	Hg(3)–O(3)♯6	2.492(12)
U(1)–O(3)♯1	2.358(13)	Hg(3)–O(4)♯4	2.595(12)
U(1)–O(2)♯4	2.371(12)	As(1)–O(1)	1.661(12)
Hg(1)–O(5)	2.018(14)	As(1)–O(2)	1.685(12)
Hg(1)–O(5)♯1	2.018(14)	As(1)–O(3)	1.692(12)
Hg(2)–O(7)	2.015(13)	As(1)–O(4)	1.718(13)
Long Hg–O bond distances (Å)			
Hg(1)–O(2)	3.243(15)	Hg(2)–O(5)	2.717(15)
Hg(1)–O(4)	2.790(15)	Hg(2)–O(6)	2.760(15)
Hg(1)–O(9)	2.841(15)	Hg(2)–O(2)	2.737(15)
Angles (deg)			
O(5)–Hg(1)–O(5)♯1	180	O(3)♯6–Hg(3)–O(4)♯4	144.9(4)
O(7)–Hg(2)–O(6)	178.1(5)	Hg(1)–O(5)–Hg(3)	110.1(6)
O(4)–Hg(3)–O(6)	157.9(5)	Hg(2)–O(7)–U(1)♯2	124.3(6)
O(4)–Hg(3)–O(5)	126.4(5)	Hg(2)–O(7)–U(1)	115.8(6)
O(6)–Hg(3)–O(5)	75.7(5)	As(1)–O(3)–Hg(3)♯6	117.3(6)
O(4)–Hg(3)–O(3)♯6	91.1(4)	U(1)♯1–O(3)–Hg(3)♯6	105.2(5)
O(6)–Hg(3)–O(3)♯6	90.9(5)	Hg(2)–O(6)–Hg(3)	113.1(6)
O(5)–Hg(3)–O(3)♯6	86.9(5)	As(1)–O(4)–Hg(3)	123.7(7)
O(4)–Hg(3)–O(4)♯4	78.4(5)	As(1)–O(4)–Hg(3)♯4	126.0(6)
O(6)–Hg(3)–O(4)♯4	111.3(5)	Hg(3)–O(4)–Hg(3)♯4	101.6(5)
O(5)–Hg(3)–O(4)♯4	73.5(4)		

Symmetry transformations used to generate equivalent atoms: ♯1 $-x+1,-y,-z+1$; ♯2 $-x,-y-1,-z$; ♯3 $x-1,y-1,z$; ♯4 $-x+1,-y+1,-z+1$; ♯5 $-x,-y,-z$; ♯6 $-x+2,-y+1,-z+1$; ♯7 $x+1,y+1,z$.

Table 3
Atomic coordinates ($\times 10^4$) and equivalent isotropic displacement parameters ($Å^2 \times 10^3$) for $[Hg_5O_2(OH)_4][(UO_2)_2(AsO_4)_2]$ (**HgUAs-1**).

	x	y	z	U(eq)[a]
Hg(1)	1/2	0	1/2	16(1)
Hg(2)	2415(1)	−626(1)	323(1)	13(1)
Hg(3)	5690(1)	3871(1)	3202(1)	14(1)
U(1)	60(1)	−3740(1)	2092(1)	9(1)
As(1)	9360(3)	7737(3)	6044(2)	9(1)
O(1)	0390(20)	7920(20)	4691(15)	14(3)
O(2)	9388(19)	0089(19)	7363(14)	11(2)
O(3)	0766(18)	6400(20)	7009(14)	10(2)
O(4)	6821(19)	6576(19)	5260(14)	11(2)
O(5)	5400(20)	200(20)	3035(17)	19(3)
O(6)	4390(20)	2080(20)	775(15)	14(3)
O(7)	430(20)	−3200(20)	−75(16)	15(3)
O(8)	−2700(20)	−3650(20)	1545(16)	18(3)
O(9)	2770(20)	−3850(20)	2687(14)	15(3)

[a] $U(\text{eq}) = 1/3[U22+1/\sin^2\beta(U11+U33+2U13\cos\beta)]$.

consistent with the corresponding average single crystal data of 1.820(15) Å [32]. Bands observed lower than 300 cm^{-1} are assigned to the ν_2 (δ) UO_2^{2+} (ν (U–O) and δ (U–O) vibrations) as well as the Hg–O bonds. The bands at 884 and 842 cm^{-1} are assigned to the AsO_4^{3-} antisymmetric stretching modes. The AsO_4^{3-} symmetric stretching mode is found at 628 cm^{-1}. The bands near 507 cm^{-1} can be assigned to AsO_4^{3-} bending [33].

Fluorescence spectroscopy: The emission of green light from uranyl compounds excited by long-wavelength UV light has been known for centuries. Fluorescence from uranyl compounds can be identified from the vibronic fine-structure characteristic of the UO_2^{2+} moiety [34]. Uranyl fluorescence typically has a characteristic five peak spectrum relating to the $S_{11} \rightarrow S_{00}$ and $S_{10} \rightarrow S_{0v}$

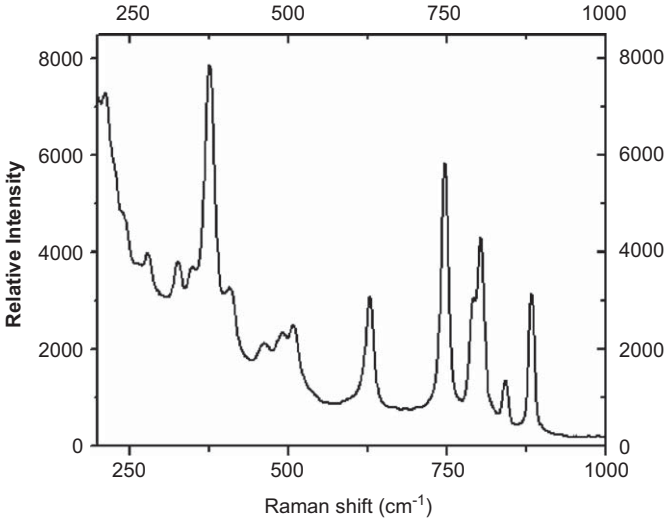

Fig. 5. Raman spectrum of $[Hg_5O_2(OH)_4][(UO_2)_2(AsO_4)_2]$ (**HgUAs-1**).

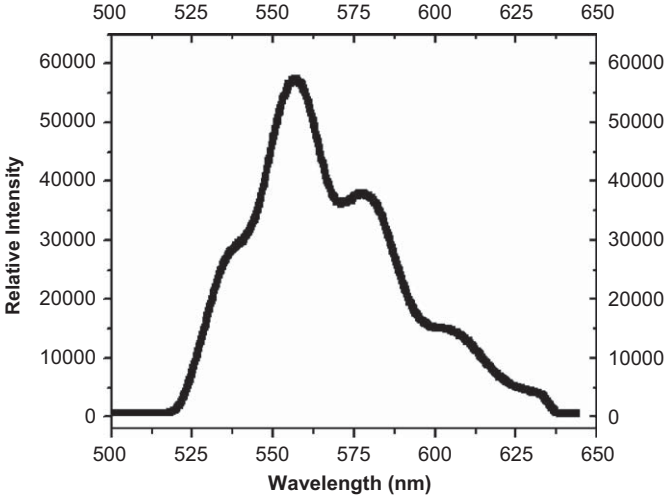

Fig. 6. Fluorescence spectrum of $[Hg_5O_2(OH)_4][(UO_2)_2(AsO_4)_2]$ (**HgUAs-1**).

($v = 0$–4) electronic and vibronic transitions, and for $UO_2(NO_3)_2 \cdot 6H_2O$ the most intense peak ($S_{10} \rightarrow S_{00}$) is position at 508 nm [35–37]. The vibronic transitions for **HgUAs-1** are somewhat broad, and five transitions are discernable, as shown in Fig. 6.

4. Conclusions

A new member of the $M/UO_2^{2+}/AsO_4$ family, $[Hg_5O_2(OH)_4][(UO_2)_2(AsO_4)_2]$ (**HgUAs-1**), has been synthesized and structurally and spectroscopically characterized. This compound is a rare of example of a mercury uranyl oxoanion system, and the mercury oxide/hydroxide layers differ substantially from the cationic layers typically found in uranyl compounds.

Appendix A. Supplementary material

Supplementary data associated with this article can be found in the online version at doi:10.1016/j.jssc.2009.03.032.

References

[1] A.J. Locock, P.C. Burns, Can. Mineral. 41 (2003) 489.
[2] A.J. Locock, P.C. Burns, Can. Mineral. 41 (2003) 91.
[3] A.J. Locock, P.C. Burns, Am. Mineral. 88 (2003) 240.
[4] A.J. Locock, P.C. Burns, J. Solid State Chem. 163 (2002) 275.
[5] P.C. Burns, Am. Mineral. 85 (2000) 801.
[6] P.C. Burns, M.L. Miller, R.C. Ewing, Can. Mineral. 34 (1996) 845.
[7] P.C. Burns, in: P.C. Burns, R. Finch (Eds.), Uranium: Mineralogy, Geochemistry and the Environmen, Mineralogical Society of America, Washington, DC, 1999 (Chapter 1).
[8] A.J. Locock, P.C. Burns, J. Solid State Chem. 177 (2004) 2675.
[9] P.C. Burns, Can. Mineral. 43 (2005) 1839.
[10] (a) T.A. Sullens, R.A. Jensen, T.Y. Shvareva, T.E. Albrecht-Schmitt, J. Am. Chem. Soc. 126 (2004) 2676;
(b) K.A. Kubatko, P.C. Burns, Inorg. Chem. 45 (2006) 10277.
[11] E.V. Alekseev, S.V. Krivovichev, W. Depmeier, O.I. Siidra, K. Knorr, E.V. Suleimanov, E.V. Chuprunov, Angew. Chem. Int. Ed. 45 (2006) 7233.
[12] S.V. Krivovichev, C.L. Cahill, P.C. Burns, Inorg. Chem. 41 (2002) 34.
[13] A.J. Locock, P.C. Burns, T.M. Flynn, Can. Mineral. 42 (2004) 1699.
[14] T.Y. Shvareva, T.A. Sullens, T.C. Shehee, T.E. Albrecht-Schmitt, Inorg. Chem. 44 (2005) 300.
[15] T.Y. Shvareva, S. Skanthakumar, L. Soderholm, A. Clearfield, T.E. Albrecht-Schmitt, Chem. Mater. 19 (2007) 132.
[16] T.Y. Shvareva, J.V. Beitz, E.C. Duin, T.E. Albrecht-Schmitt, Chem. Mater. 17 (2005) 6219.
[17] K. Brodersen, G. Liehr, D. Prochaska, G. Schottner, Z. Anorg. Allg. Chem. 521 (1985) 215.
[18] K. Brodersen, G. Liehr, G. Schottner, Z. Anorg. Allg. Chem. 529 (1985) 15.
[19] N.V. Pervukhina, G.V. Romanenko, S.V. Borisov, S.A. Magarill, N.A. Palchik, J. Struct. Chem. 40 (1999) 461.
[20] F.C. Hawthorne, C. Mark, P.K.S. Gupta, Am. Mineral. 79 (1994) 1199.
[21] K. Brodersen, G. Liehr, G. Schottner, Z. Anorg. Allg. Chem. 531 (1985) 158.
[22] M. Weil, Z. Anorg. Allg. Chem. 631 (2005) 829.
[23] M.A. Cooper, F.C. Hawthrone, Can. Mineral. 41 (2003) 1173.
[24] G.M. Sheldrick, SHELXTL PC, Version 6.12, An Integrated System for Solving, Refining, and Displaying Crystal Structures from Diffraction Data, Siemens Analytical X-ray Instruments, Inc., Madison, WI, 2001.
[25] G.M. Sheldrick, SADABS 2001, Program for absorption correction using SMART CCD based on the method of Blessing: Blessing, R.H., Acta Crystallogr. A 51 (1995) 33.
[26] P.C. Burns, R.C. Ewing, F.C. Hawthorne, Can. Mineral. 35 (1997) 1551.
[27] V.N. Serezhkin, N.V. Boiko, V.K. Trunov, J. Struct. Chem. 23 (1982) 270.
[28] N.E. Brese, M. O'Keeffe, Acta Crystallogr. B 47 (1991) 192.
[29] I.D. Brown, The Chemical Bond in Inorganic Chemistry: The Bond Valence Model, Oxford University Press, London, 2002.
[30] I.D. Brown, D. Altermatt, Acta Crystallogr. B 41 (1985) 244.
[31] A.J. Locock, P.C. Burns, J. Solid State Chem. 176 (2003) 18.
[32] J.R. Bartlett, R.P. Cooney, J. Mol. Struct. 193 (1989) 295.
[33] K. Nakamoto, Infrared and Raman Spectra of Inorganic and Coordination Compounds. Part A: Theory and Applications in Inorganic Chemistry, fifth ed., Wiley-Interscience Publication, 1997.
[34] R.G. Denning, J.O.W. Norris, I.G. Short, T.R. Snellgrove, D.R. Woodwark, Lanthanide and Actinide Chemistry and Spectroscopy, in: N.M. Edelstein (Ed.), ACS Symposium Series No. 131, American Chemical Society, Washington, DC, 1980 (Chapter 15).
[35] L.A. Borkowski, C.L. Cahill, Cryst. Growth Des. 10 (2006) 2241.
[36] X. Kong, Y. Ren, L. Long, R. Huang, L. Zheng, Inorg. Chem. Commun. 10 (2007) 894.
[37] M. Frisch, C.L. Cahill, Dalton Trans. 39 (2006) 4679.